PROTEINS: Structure, Function, and Bioinformatics 66:528–537 (2007)

Modeling the Interaction Between Aldolase and the Thrombospondin-Related Anonymous Protein, a Key Connection of the Malaria Parasite Invasion Machinery

Carlos A. Buscaglia,[1*] Wim G. J. Hol,[2] Victor Nussenzweig,[1] and Timothy Cardozo[3]
[1]*Michael Heidelberg Division of Pathology of Infectious Diseases, Department of Pathology, New York University School of Medicine (NYSoM), New York*
[2]*Department of Biochemistry, Howard Hughes Medical Institute, Biomolecular Structure Center, University of Washington, Seattle, Washington*
[3]*Department of Pharmacology, New York University School of Medicine (NYSoM), New York*

ABSTRACT **A complex molecular motor empowers substrate-dependent motility and host cell invasion in malaria parasites. The interaction between aldolase and the transmembrane adhesin thrombospondin-related anonymous protein (TRAP) transduces the motor force across the parasite surface. Here, we analyzed this interaction by using state-of-the-art flexible docking. Besides algorithms to account for induced fit in the side-chains of the *Plasmodium falciparum* aldolase (PfAldo) structure, we used additional *in silico* receptors modeled upon crystallographic structures of evolutionarily related aldolases to incorporate enzyme backbone flexibility, and to overcome structure inaccuracies due to the relatively low resolution (3.0 Å) of the genuine PfAldo structure. Our results indicate that, in spite of multiple intermolecular contacts, only the six C-terminal residues of the TRAP cytoplasmic tail bind in an ordered manner to PfAldo. This portion of TRAP targets the PfAldo active site, with its n-1 Trp residue, which is essential for this interaction, buried within the PfAldo catalytic pocket. Docking of a TRAP peptide bearing a Trp to Ala mutation rendered the lower energy configurations either bound weakly outside the active site or not bound to PfAldo at all. The position of the bound TRAP peptide, and particularly the close proximity between the carbonyl of its n-2 Asp residue and the experimentally determined position of the phosphate-6 group of fructose 1,6-phosphate bound to mammalian aldolases, predicts an inhibitory effect of TRAP on catalysis. Enzymatic and TRAP-binding assays using mutant PfAldo molecules strongly support the overall structural model. These results might provide the initial framework for the identification of novel antiparasitic compounds. Proteins 2007;66:528–537.** © 2006 Wiley-Liss, Inc.

Key words: Plasmodium; apicomplexa; flexible docking; WASp; molecular motor; mutagenesis

INTRODUCTION

Fructose 1,6-biphosphate (F1,6P) aldolase mediates the reversible cleavage of F1,6P to dihydroxyacetone phosphate (DHAP) and glyceraldehyde 3-phosphate (G3P). Class I aldolases are homotetrameric enzymes present in all groups of organisms that catalyze their reaction through the formation of a Schiff-base with the substrate, whereas Class II aldolases, restricted to algae, yeast, and eubacteria, require a divalent metal ion as a cofactor.[1] The crystal structures of several Class I aldolases have been solved, including those from *Plasmodium falciparum* (PfAldo[2]), *Leishmania mexicana*,[3] *Trypanosoma brucei*,[3] *Drosophila melanogaster*,[4] and the human isoforms present in muscle,[5] liver,[6] and brain tissue.[7] Crystallographic studies of covalent reaction intermediates and aldolases trapped in complex with F1,6P, DHAP, or competitive inhibitors have also been reported.[8–11] All Class I aldolases crystallized so far display the same basic architecture commonly referred to as triose phosphate isomerase (TIM)-barrel. In this architecture, each subunit of the tetramer folds into a repetitive eight-fold βα motif, with the active site located in the center and only accessible from one side.[12] Attached to this core by a flexible hinge, the C-terminal ~20 residues of each subunit delineate a flexible armlike structure that hovers over the enzyme surface, sometimes contacting the active site.[13,14] The catalytic amino acids, including the nucleophilic Schiff-base forming residue and the basic residues binding to the phosphate groups of F1,6P, are extremely conserved.[1]

Abbreviations: DHAP, dihydroxyacetone phosphate; F1,6P, fructose 1,6-biphosphate; G3P, glyceraldehyde 3-phosphate; PDB, protein database; PfAldo, *Plasmodium falciparum* aldolase; TIM, triose phosphate isomerase; TRAP, thrombospondin-related anonymous protein; WASp, Wiskott–Aldrich Syndrome protein.

The Supplementary Material referred to in this article can be found at http://www.interscience.wiley.com/jpages/0887-3585/suppmat/

Grant sponsors: National Institutes of Health (NIH), New York University School of Medicine.

*Correspondence to: Carlos A. Buscaglia, Instituto de Investigaciones Biotecnológicas-Instituto Tecnológico de Chascomús (IIB-INTECH), Universidad Nacional de General San Martín-CONICET; Av. Gral Paz y Albarellos, Predio INTI, edificio 24, San Martín (1650), Buenos Aires, Argentina. E-mail: buscac01@med.nyu.edu

Received 19 May 2006; Revised 22 August 2006; Accepted 20 September 2006

Published online 7 December 2006 in Wiley InterScience (www.interscience.wiley.com). DOI: 10.1002/prot.21266

TABLE I. Library of Crystallographic Aldolase Structures Used for the Docking Experiments

PDB ID[a]	Enzyme origin	Resolution (Å)	Identity[b]	Cα RMSD to PfAldo[c]	Complex[d]	Ref.
1A5C[e]	*P. falciparum*	3.00	100	0.00	–	2
1EPX	*L. mexicana*	1.80	46	8.75	–	3
1ADO	Rabbit muscle	1.90	57	12.60	–	14
1F2J	*T. brucei*	1.90	47	8.74	–	3
1FBA	*D. melanogaster*	1.90	56	12.44	–	4
1ALD	Human muscle	2.00	56	12.43	–	5
6ALD	Rabbit muscle	2.30	56	12.50	F1,6P	9
1J4E	Rabbit muscle	2.65	56	12.49	DHAP	10
4ALD	Human muscle	2.80	56	12.54	F1,6P	8

[a]Protein database identification code.
[b]Amino acid identity values (in percentage) to the *P. falciparum* aldolase.
[c]Cα root-mean-square deviation (RMSD) values between the indicated aldolase structure and *P. falciparum* aldolase monomer A.
[d]The aldolase crystallographic structure has been solved in the presence of the indicated molecule.
[e]Contains the structure of two aldolase monomers, which were independently used for docking.

In addition to its glycolytic role, aldolase binds to several proteins including actin[15,16] and tubulin,[17] indicating that, for some of these polypeptide ligands, it can function as an indirect anchor to the cytoskeleton (reviewed in Refs. 7 and 18). Indeed, in the pathogens *Toxoplasma gondii* and *Plasmodium berghei*, aldolase bridges the cortical actin filaments to the cytoplasmic tail of transmembrane adhesins from the thrombospondin-related anonymous protein (TRAP) family.[19,20] An unusual myosin promotes the backward movement of these actin filaments, leading to a redistribution of aldolase-TRAP complexes along the parasite surface.[21,22] The molecular components and the overall arrangement of this machinery, which is critical for parasite motility and host cell invasion, are evolutionary conserved across the phylum Apicomplexa.[23,24] TRAP analogous proteins, displaying aldolase-binding sequences on their cytoplasmic tails and different adhesive motifs on their extracellular portions, are thought to provide the connection between the intracellular actin-myosin motor and the various host cell receptors recognized by the different apicomplexan parasites, including the three invasive stages of Plasmodium: sporozoites, ookinetes, and merozoites.[24–28] The interaction between TRAP family proteins and aldolase, hence, constitutes an appealing drug target to treat malaria and other human and livestock diseases.

Even though the TRAP-binding site on aldolase remains elusive, some observations suggest that TRAP targets the enzyme catalytic pocket. For example, the presence of low micromolar concentrations of F1,6P, DHAP, or G3P in the medium abolishes the binding of TRAP to aldolase.[18,19] This inhibitory role of aldolase substrate/products has been documented also for other mammalian proteins that bind to aldolase via "TRAP-like" sequences such as the Wiskott–Aldrich syndrome protein (WASp),[18] and the erythrocyte anion exchanger Band 3.[29] Furthermore, a model of a complex between rabbit muscle aldolase and a synthetic Band 3 peptide indicates that their binding is stabilized by ionic interactions involving the positively charged residues from the enzyme active site.[29] In the present work, we undertook a flexible peptide computational docking study followed by biochemical and mutagenesis approaches to analyze the binding location of the TRAP peptide on Plasmodium aldolase.

MATERIALS AND METHODS

Library of Crystallographic Structures Used as Receptors for Docking

To account for receptor flexibility and structure inaccuracies due to the relatively low resolution (3.0 Å) of the PfAldo available structure,[2] we searched for highly homologous crystallographic structures belonging to the same protein family at http://scop.mrc-lmb.cam.ac.uk/scop.[30] Of these, only the enzyme complexes with F1,6P or DHAP and all high resolution ($\leq$2.0 Å), nonmutant structures were selected (Table I). The PfAldo structure contains two monomers, which were independently used for docking. In the case of complexed structures, the F1,6P or DHAP molecules were removed prior to docking.

Model Building and Refinement

PfAldo 3D homology models were built for each aldolase structure to be used as *in silico* docking receptors, using the following steps with the ICM program.[31] Briefly, (1) the sequence alignment corresponding to the superimposition of each 3D structure from Table I (the template) with the PfAldo wild type apo-structure was extracted using the align 3D command in ICM, (2) an extended polypeptide chain with idealized covalent geometry[32] was built for each template, (3) torsion angles for the aligned portions of the backbone and identical aligned residues were assigned to those in the template structure, (4) the most likely rotamer was assigned to nonidentical aligned residues and near-extended backbone torsion values were assigned to the loops, (5) the sum of the physical energy and quadratic restraints between corresponding atoms in the model and template structures were iteratively minimized, reducing the strength of the restraint potential with each iteration,

and (6) nonidentical side-chains and loops were subjected to Biased-Probability Monte Carlo sampling[32] to produce the lowest energy structure matching the template coordinates. The final Cα root-mean-square deviation (RMSD) for each model was less than 0.5 Å to the PDB structure for matched segments.

Flexible Model of the TRAP Ligand

All-atom models of the various TRAP peptides (the ligands) with charged N- and C-termini were used. Internal coordinates (bond length and angle, torsion angle, and phase angle) describe the ligands, and six virtual variables describe the orientation of each ligand with respect to rotations and translations in space. Bond lengths and angles were fixed to ideal values, but torsion, phase, and virtual variables were sampled during docking, making the ligand fully flexible within the grid.

Ab Initio Flexible Peptide Docking by Grid Potentials

TRAP models were docked into grid potentials derived from each PfAldo model using a stochastic global optimization in internal coordinates with pseudo-Brownian and collective probability-biased random moves as implemented in the ICM 3.0 program. Five types of potentials[33] for the ligand–receptor interaction energy were precomputed using the following equation

$$E_{\mathrm{TRAP-PfAldo}} = E_{\mathrm{Cvw}} + E_{\mathrm{Hvw}} + 0.87E_{\mathrm{hb}} + 3.68E_{\mathrm{el}} + 1.58E_{\mathrm{hb}}$$

on a rectilinear grid with 0.5 Å spacing that fills a 34 Å × 34 Å × 25 Å box containing the active site and surrounding surfaces of each receptor (~70% of the aldolase surface constituting the central barrel and the entire surface of the open end of the TIM-barrel). The weights multiplying E_{hb}, E_{el}, and E_{hp} were obtained from a previous study.[34] These weights are derived from the largest known set of peptide receptor complexes used in a systematic grid docking study using an approach equivalent to ours. In addition, these weights are used only for the grid docking portion of the search, which is intended primarily to generate a diverse set of promising poses for full atom refinement as described below. The van der Waals (vdW) grid potentials for nonhydrogen (E_{Cvw}) and hydrogen (E_{Hvw}) atoms were calculated from a vdW energy, which was smoothed by introducing a cutoff value $E_{\mathrm{vwmax}} = 3$ kcal/mol[35] to reduce the extreme sensitivity of the vdW potential to small conformational changes, and to speed convergence of local minimization of the energy function. The hydrogen bonding (E_{hb}) and hydrophobic (E_{hp}) potentials were calculated as described,[35] and the electrostatic energy (E_{el}) was calculated using a distance-dependent dielectric constant = $4r$. The TRAP-PfAldo intermolecular energy calculated using these grid potentials was added to the peptide intramolecular energy, E_{peptide}, which was calculated using the truncated vdW energy with a cutoff $E = 7$ kcal/mol, the distance-dependent dielectric electrostatic term, ECEPP/3,[36] hydrogen-bonding and torsional potentials, and a side-chain entropic term proportional to the fractional solvent accessible surface area (SASA).[37] All free torsion angles of docked TRAP peptides were randomized with the amplitude of 180° to generate a starting conformation. The output of each grid docking simulation was a set of 40 lowest energy accepted conformations differing by 30° RMSD in torsion angle coordinates (to prevent oversampling of nearby points in coordinate space).[38]

All-Atom Refinement and Reranking of Combined Search

Each of the 40 lowest energy conformations from each docking simulation was locally optimized with the surrounding side-chains of the receptor using a more realistic physical energy function derived from an all-atom model of both the ligand and the receptor. For each conformation, a copy was made and a quadratic restraint energy

$$E_{\mathrm{restraint}} = kR_{ij}{}^2,$$

where R is the distance between restrained atoms in angstroms (Å) and k is a strength constant = 10 kcal/(mol × Å^2), was imposed between corresponding Cα atoms in the ligand and the copy, restricting the refinement of each conformation to the side-chains at the interface between TRAP and PfAldo. ICM Biased-Probability Monte Carlo sampling[32] was then applied to sample these interface side-chain χ angles, defined as the torsion angles within 10 Å from the shared boundary in either TRAP or PfAldo. Conformations were sampled according to a Metropolis criterion[39] with a temperature of 700 K followed by up to 2000 steps of conjugate gradient minimization after each stochastic move. Torsion angles of the TRAP backbone were not globally sampled, but were included in the conjugate gradient minimization space. The energy function, which uses ECEPP/3 force field parameters,[36] was

$$E = E_{\mathrm{vw}} + E_{\mathrm{to}} + E_{\mathrm{el}} + E_{\mathrm{hb}} + E_{\mathrm{hb}} + E_{\mathrm{restraint}}$$

in which E_{to} and E_{hb} are the original ECEPP/3 energy functions. E_{vw} is the smoothed vdW term described above with a cutoff energy $E_{\mathrm{vwmax}} = 7$ kcal/mol. The electrostatics term E_{el} was calculated using the boundary element method with ECEPP/3 atomic charges and an internal dielectric constant of 4. The hydrophobic term E_{hp} was calculated as the product of a surface tension parameter 12 cal/(mol × Å^2) and the molecule's SASA. The side-chain entropy term

$$E_{\mathrm{el}} = T \times S_{\mathrm{max}} \times A/A_{\mathrm{max}}$$

is proportional to the total SASA of the side-chain atoms A, in which $T = 300$ K, A_{max} is the total SASA of the atoms with the residue between two glycine residues in an extended peptide conformation, and S_{max} was calcu-

lated using approximate rotamer distributions.[32] This configuration of sampling and energy function resulted in relatively small conformational changes that primarily reduced steric clashes caused by the steeper all-atom vdW's potential as compared to the smoother grid version of the potential. The full atom refinement uses a broadly validated computational chemistry (as opposed to empirical/statistical) energy function that has previously correctly predicted ab initio and loop peptide structures in advance of experimental solution.[32] The final ranking and identification of the convergent solution was more dependent on this latter, fully transferable energy function and less on the more empirically weighted grid potential solutions. Calculation for each conformation took an average of 10–12 CPU hours on a 1.67 GHz PowerPC G4 chip (~900,000 function calls). The lowest energy score and conformation from each of the nine sets of 40 lowest grid docking conformations (n = 360) were then combined and ranked according to the all-atom energy (Suppl. Table I). The lowest energy conformation was chosen as the final docking solution for that run.

Definition of Convergence

It is important to verify that the ICM stochastic energy minimization has converged, since otherwise the global minimum may be missed and the results will not be reproducible from independent simulations. In this case, grid docking followed by all-atom refinement and reranking was performed multiple times in parallel starting from different ligand conformations, and convergence was defined as two or more parallel simulations identifying the same lowest energy conformation. After six parallel runs, the same conformation of the 6mer TRAP peptide was identified by two independent parallel runs. This convergent solution was also the lowest energy conformation for all the parallel runs. Prediction of the W to A mutant TRAP peptide converged after eight runs. Prediction of the 24mer TRAP peptide never converged.

Aldolases

Mutations on PfAldo[40] were introduced by PCR and checked by DNA sequencing. Glutathione *S*-transferase (GST)-tagged and histidine $(His)_6$-tagged PfAldo variants were expressed in *Escherichia coli*, purified as described,[41] and quantified using the Micro BCA™ protein assay kit (Pierce). For the binding assays, the GST-tag was removed by in-column treatment with activated Factor X (New England Biolabs).

TRAP/WASp Molecules

Peptides derived from *P. falciparum* TRAP, human WASp, and *Plasmodium yoelii* CS protein, as well as the GST-fusion proteins spanning the aldolase-binding sites of *P. berghei* TRAP and human WASp, and their mutational derivatives, have been described.[18]

Aldolase Binding Assays

White polystyrene ELISA microplates (Nunc) were coated with 1 nmol/well of TRAP peptide in carbonate buffer 50 m*M* pH 9.6, blocked with 200 μL of ELISA buffer (Imidazole acetate 10 m*M* pH7.3, 50 m*M* KCl, 0.2% Tween-20) supplemented with 3% BSA, and probed with dilutions of different PfAldo mutants in the same buffer. Binding was revealed by the addition of a rabbit antibody against the C-terminal peptide of *P. berghei* aldolase[19] followed by HRP-conjugated antirabbit IgG (Amersham Biosciences). After five washings, plates were rinsed with 100 μL of ELISA buffer without Tween-20, and added with 100 μL of the chemiluminescent substrate ECL (Amersham) diluted 1:5 in the same buffer. Signal intensity was quantified using Image J program (http://rsb.info.nih.gov/ij).

Aldolase Activity and Inhibition Assays

Aldolase activity was assayed by coupling the F1,6P cleavage to the TIM/G3P dehydrogenase reaction, and continuous measuring of NADH consumption at 340 nm.[19] For the inhibition assays, a two-step protocol was followed. Peptides or GST-fusion molecules diluted in 50 μL of PBS-BSA 0.01% were preincubated at room temperature with 250 ng of wild type PfAldo diluted in 50 μL of EDTA 0.1 m*M*, Tris–HCl 50 m*M* pH 7.5. After 15 min, the mixture was transferred to 0.9 mL of F1,6P 50 μ*M*, NADH 0.1 m*M*, 10.7 U of TIM, 0.91 U of G3P dehydrogenase, EDTA 0.1 m*M*, Tris–HCl 50 m*M* pH 7.5, Tween 20 0.2%, BSA 0.01%, and absorbance at 340 nm recorded every 3 min. For the specific activity assays, 2 m*M* of F1,6P were constantly used. One unit was defined as the amount of aldolase required to cleave 1 μmol of F1,6P per minute in these conditions. Mean values were compared to the corresponding control values by using the Student's t test.

Size Fractionation

Partially purified $(His)_6$-tagged PfAldo proteins were dialyzed against PBS, and size-fractionated on a Superdex 200 HR 10/30 column (Amersham), previously calibrated based on the elution positions for molecular markers. One-milliliter fractions were collected, and used to coat clear ELISA plates (100 μL/well). After blocking with TBS, supplemented with 0.1% Tween-20 and 3% nonfat milk, plates were probed with antibodies to full-length PfAldo.[19]

RESULTS

In Silico *Docking of the TRAP Peptide to Aldolase*

We previously mapped the aldolase-binding site in TRAP to its C-terminal ~24 residues.[18,19] On the basis of these observations, we undertook a flexible docking approach of the corresponding P. berghei-derived 24mer peptide (NH_2-VMADDEKGIVENEQFKLPEDNDWN-COOH) to PfAldo and different PfAldo models built upon available crystallographic structures of different aldolases (Table

I). The vast majority of the lowest energy configurations bound the C-terminal portion of the TRAP peptide to the PfAldo active site (data not shown). The N-terminal 18–20 residues of this peptide, however, varied significantly between the conformations, and convergence (see Materials and Methods) was never achieved for this prediction. These results indicated that there is a strong interaction between the C-terminal 4–6 residues of TRAP and the PfAldo active site but that one of the following represented an insurmountable obstacle to structural confirmation of the interaction with the 24mer peptide: (1) the computational burden of the prediction of the full 24mer peptide complex is too high; (2) the N-terminal 18–20 residues of the 24mer peptide are disordered when bound to aldolase; or (3) the PfAldo conformation, when bound to the TRAP peptide, differs too much outside of the active site when considering each of the structural models used.

To bypass these limitations, we undertook a similar flexible docking approach but using only the C-terminal 6 residues of TRAP (EDNDWN). As mentioned, this portion of the TRAP cytoplasmic tail showed some propensity to dock convergently to the active site when using the 24mer peptide and was previously demonstrated to contribute the most to the aldolase binding.[18] In this case, the same lowest energy configuration resulted from two simulations starting from different ligand conformations (i.e. convergence was achieved) [Fig. 1(A)]. The exact coordinates for this configuration are provided as supplemental data. It is not expected that this configuration is identical in its fine details to the native interaction mode of TRAP with aldolase in part, because the affinity of the interaction may be low for this hexamer peptide, and therefore the dominant mode may be difficult to distinguish from energetically reasonable alternative modes. However, additional conformations showing similar predicted energy of interaction in the docking were also all similar in their general backbone structure and N- to C-orientation in the binding location on aldolase, with the differences primarily attributable to the side-chains and minor deviations in the backbone trace. The 30 lowest energy configurations docked to the enzyme active site, with their extreme C-termini buried within the catalytic pocket [Fig. 1(B)]. Importantly, all of these 30 configurations, and >98% of the 200 most stable ones were obtained from uncomplexed conformations (i.e. crystallographic structures obtained in the absence of enzyme substrate or products) of the PfAldo receptor (Suppl. Table I).

Notably, almost all of the low energy conformations derived from a PfAldo receptor modeled upon a high resolution (1.8 Å: PDB code 1epx) structure of *L. mexicana* aldolase[3] (Suppl. Table I). Interestingly, this structure has a significant structural deviation from the apo-form of PfAldo in exactly the segments predicted to interact with the TRAP peptide: residues 43–70 and 310–330, both helix-loop-helix segments (Suppl. Fig. 1). A surface groove is apparent in this region in the *L. mexicana* aldolase structure that appears to accommodate the TRAP peptide and is absent from the apo form of PfAldo and the other high resolution apo-forms, which have a similar conformation as PfAldo. Conversely, aldolase 3D structures in complex with substrate ligands present a conformation that obliterates this groove completely.

The key role played by the TRAP n-1 Trp residue in the binding to PfAldo has been experimentally demonstrated.[19,20] Indeed, *P. berghei* sporozoites bearing a TRAP protein mutated solely at this residue did not glide on solid substrates or invade cells.[23] Considering this, a control docking experiment was carried out using a mutant TRAP 6mer peptide bearing an Ala instead of Trp at this position (EDNDAN). This resulted in the 10 lowest energy configurations settling in locations outside the aldolase active site (6 out of 10, Fig. 2), with 4 out of these 10 configurations not bound to the receptor at all (data not shown), indicating that the energy difference between bound and unbound forms of this mutant peptide is close to zero. These results, in conjunction with those obtained for the wild type 24mer and 6mer peptides, strongly suggest that the C-terminal 6 residues of TRAP bind to the active site of PfAldo, and that this interaction is likely driven by the sub-terminal Trp residue.

Partial Overlapping Between TRAP- and F1,6P-Binding Sites on Aldolase: Effect on Catalysis

The backbone of the lowest energy configuration obtained for the TRAP 6mer peptide closely overlays with the structure of F1,6P and DHAP obtained from enzyme-trapped complexes (Fig. 3 and data not shown). Of particular note is the position of the side-chain of the n-2 Asp residue in TRAP (EDN*D*WN; D4 in Fig. 3), which is almost juxtaposed with the 6-phosphate group of the F1,6P, and which can be thus stabilized by ionic interactions with similar aldolase residues. This suggests that the presence of TRAP should inhibit the cleavage of F1,6P catalyzed by PfAldo. In our standard aldolase activity assays, however, different TRAP peptides were unable to inhibit PfAldo activity even at high concentrations.[19] We hypothesized that this lack of inhibition might reflect significant differences in the affinity between the peptide and the F1,6P for the enzyme. To maximize the competitive chances of TRAP, we carried out aldolase inhibition assays using a two-step protocol and 40-fold less concentration of F1,6P (down to 50 μM; see Materials and Methods). Under these sub-optimal enzymatic conditions, we detected a small, dose-dependent inhibition of PfAldo activity mediated by TRAP but not by a control CS peptide (Fig. 4). Consistent with the above mentioned hypothesis, a highly related peptide derived from human WASp (NH_2-EDQAGDEDED-DEWDD-COOH), which displayed a ~20-fold increase in the apparent affinity for aldolase,[18] more efficiently inhibited PfAldo activity. Similar results were obtained when using GST-TRAP and GST-WASp recombinant fusion proteins under the same conditions (Fig. 4). The

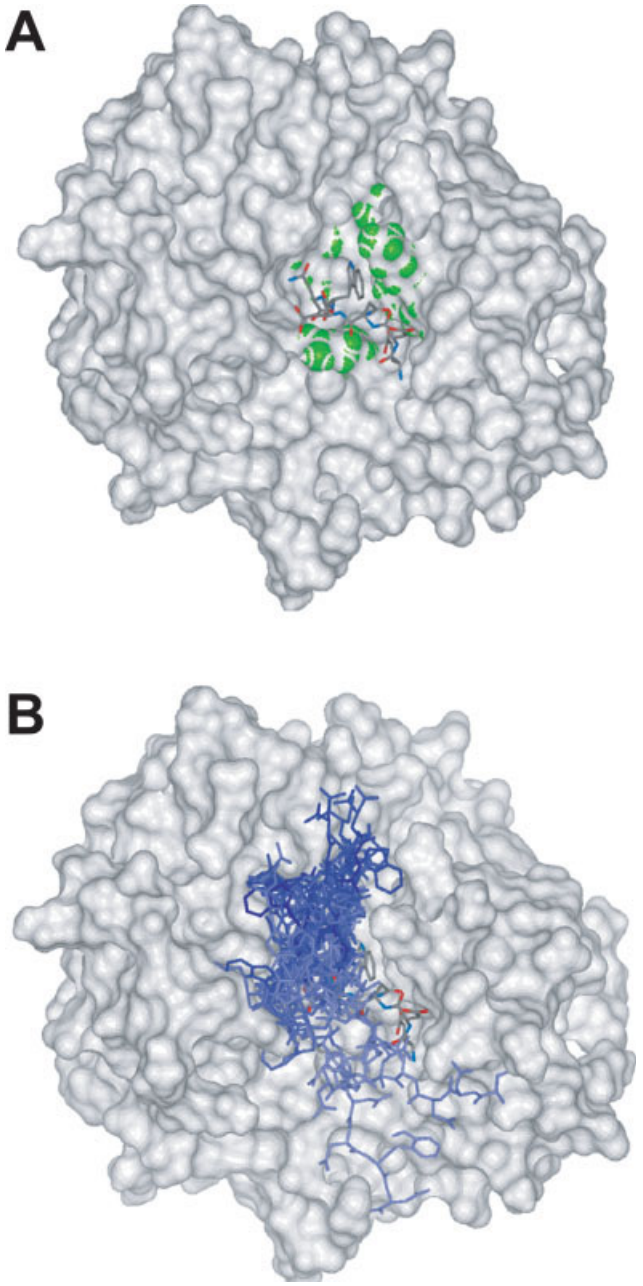

Fig. 1. The 6 C-terminal residues of TRAP dock to the aldolase active site. (**A**) The convergent lowest energy model of the TRAP 6mer peptide is shown in stick depiction over the solvent accesible surface of PfAldo. The surfaces corresponding to catalytic residues Lys 47, Arg 48, Lys 112, Lys 151, Asp 194, Lys 236, and Arg 309 are colored in green to highlight the location of the PfAldo active site. (**B**) The 30 lowest energy conformations (including the top one shown in A, only partially visible) found for the TRAP 6mer peptide are shown in blue stick depiction.

inhibitory effect exhibited by these sequences is strictly dependent on their Trp residue, as demonstrated by site-specific mutants. Furthermore, an artificial WASp molecule showing reduced aldolase affinity (WASpins[18]) also displays a reduced inhibitory effect on PfAldo catalysis as compared to GST-WASp.

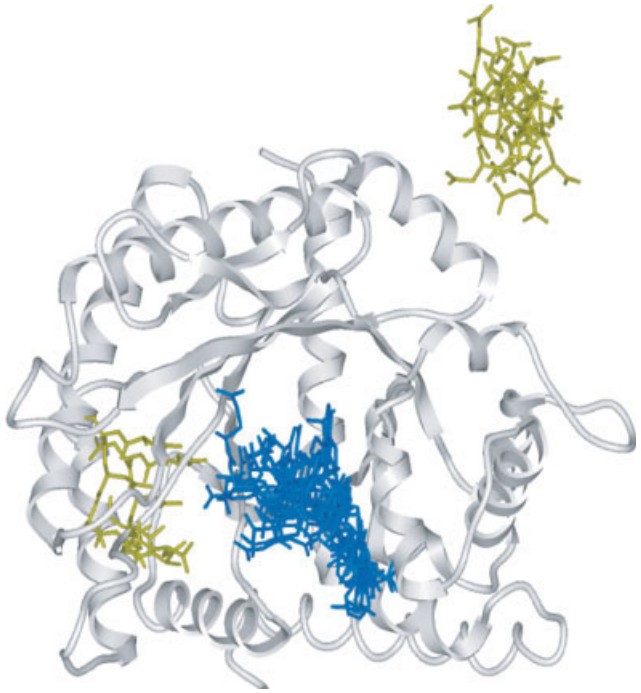

Fig. 2. Specificity of the docking of the TRAP 6mer peptide to the aldolase active site. Ribbon depiction of PfAldo showing the top 6 binding conformations (in yellow stick depictions) for the mutant TRAP peptide in which the n-1 Trp was changed to Ala. For comparison, the 10 lowest energy conformations from the wild-type TRAP 6mer peptide (blue stick depictions) are also shown.

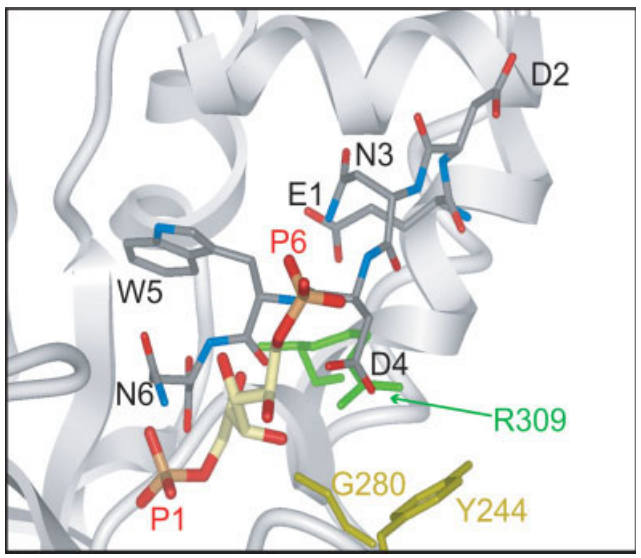

Fig. 3. Partial overlapping between TRAP- and F1,6P-binding sites on aldolase. Close view of the lowest energy configuration for the TRAP 6mer peptide superimposed with the experimentally determined conformation of F1,6P bound to human muscle aldolase (PDB ID = 4ALD). F1,6P is shown in stick depiction with standard atom coded colors (oxygen = red, phosphorous = orange, carbon = cream). Residues in TRAP (^{1}EDNDWN^{6}) are indicated in black, and the phosphate groups in F1,6P are indicated in red. The PfAldo residue R309, which interacts with both TRAP D4 and the phosphate-6 group of F1,6P is colored in green, whereas those PfAldo residues (Y244 and G280) interacting solely with the TRAP D4 residue are colored in gold.

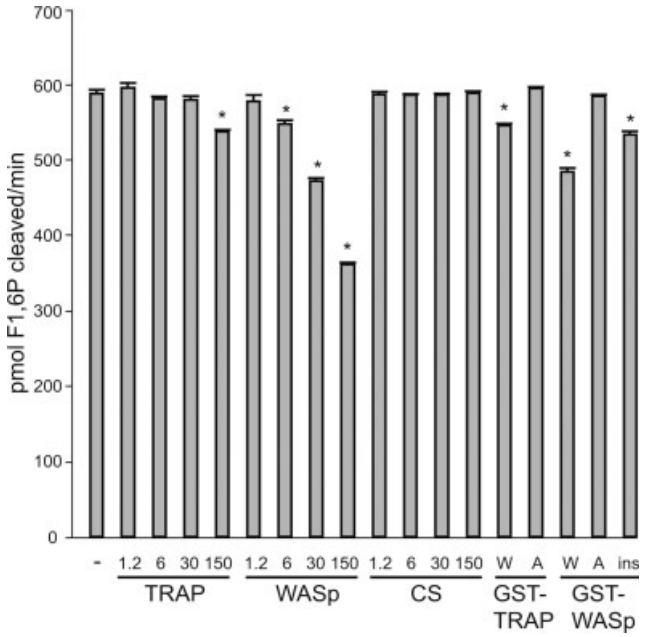

Fig. 4. Inhibition of PfAldo activity by TRAP/WASp molecules. The enzymatic activity of the wild type PfAldo was measured in the presence of the indicated molecules. The micromolar concentration of each peptide (TRAP, WASp, or CS) is shown. For GST-fusion proteins, a fixed amount (50 μM) of either the wild type (W), Trp to Ala mutant (A) or GST-WASpins (ins) mutant was used (see text for details). The indicated concentrations correspond to the preincubation step of the assay. Mean + SD values from triplicates are shown; and those significantly different ($P < 0.05$) than the mean value recorded in the absence of any addition (−) are indicated with an asterisk.

TABLE II. Effect of PfAldo Residues on Enzymatic Activity and TRAP Docking

Residue	Mutated to	Specific activity (units/mg)	Predicted contact area (Å^2)[a]
WT[b]	n/a[c]	3.25 ± 0.35	n/a
Lys 11	Glu	2.75 ± 0.36	0
Lys 12	Glu	3.21 ± 0.18	0
Lys 27	Glu	4.01 ± 0.42	0
Asp 39	Gly	<0.001[d]	39.1
Lys 47	Not done	n/a	86.0
Arg 48	Asp	0.12 ± 0.01[d]	134.6
Lys 72	Glu	2.26 ± 0.42	0
Lys 112	Asp	<0.001[d]	10.3
Lys 115	Glu	3.40 ± 0.12	0
Arg 138	Ala	3.29 ± 0.22	0
Lys 151	Asp	<0.001[d]	15.9
Glu 194	Lys	0.008 ± 0.0005[d]	17.1
Lys 236	Asp	<0.001[d]	24.0
Ser 278	Not done	n/a	44.4
Arg 309	Not done	n/a	218.0

[a]Calculated using the lowest energy conformation for the docking of the TRAP 6mer peptide.
[b]Wild type PfAldo.
[c]n/a, nonapplicable.
[d]Significantly different ($P < 0.01$) from the wild type PfAldo value.

Mapping of the TRAP-Binding Site on Aldolase by Site-Specific Mutagenesis

On the basis of the above results, we mutated different residues on the PfAldo surface, including the active site.[2] The predicted contact area with the TRAP 6mer for each of these residues, as calculated from the docking results, as well as the specific activity and quaternary structure of the ensuing PfAldo variants are indicated in Table II and Suppl. Figure 2. The TRAP binding capacity of each mutant was measured on solid phase, using as bait a TRAP 25mer peptide, and the flexible C-terminus region of PfAldo as immunological tag. Antibodies to this region do not interfere with the PfAldo-TRAP binding.[19] Overall, mutations affecting catalytic residues ($n = 6$) have a significantly increased impact in the TRAP binding than control mutations ($n = 6$) carried out on noncatalytic residues [Fig. 5(A)]. Within the latter group, the only residue rendering a significant effect (~75% reduction upon mutation) in the binding to TRAP was Arg 138. Since the specific activity of this mutant is not affected (Table II), it is possible that Arg 138 might be contacting additional TRAP residues not included in the 6mer peptide used for docking. In sharp contrast, five out of six active site mutants yielded 85–99.9% reduction in their TRAP binding. Mutation of Arg 48, for instance, completely abolished TRAP binding, which correlates with its predicted extensive contact area with TRAP that includes the n-1 Trp and the side-chains of n-3 Asn and n-5 Glu residues [Fig. 5(B,C)]. Another critical residue in terms of TRAP binding is Glu 194, which exhibits multifunctional roles in aldolase catalysis.[42] According to the docking assays, the nitrogen of the amide group of the C-terminal Asn in TRAP is close to and oriented toward the negatively charged carbonyl side-chain group of Glu 194 [Fig. 5(B,C)]. Even though the predicted contact area between TRAP and Glu 194 is only 17.1 Å^2, its mutation to Lys would likely disrupt this electrostatic contact, and since Lys has a longer side-chain than Glu, this mutation may also produce an atomic clash with the peptide. PfAldo residues Lys 112 and Lys 151 are predicted to contact the indole ring of the n-1 Trp residue, and both of them showed dramatically reduced binding (~95% reduction) upon mutation. Mutation of the Schiff-base forming residue Lys 236, which is buried at the bottom of the active site pocket and solely reached by the TRAP peptide C-terminal Asn, has an intermediate impact on the TRAP binding (~85% reduction). Finally, Asp 39 has a minor effect on the TRAP binding (~41% reduction upon mutation), although its contact area is predicted to be quite extensive (39.1 Å^2). To further test these results, not-so-drastic mutations were produced for some of the already evaluated residues: Arg 48 to Gly, Lys 151 to Gly, Lys 11 to Ala, and Lys 72 to Ala. The binding of these new mutants was indistinguishable from that of the original mutations shown in Figure 5(A) (data not shown), thus ruling out a major role of nonspecific ionic repulsion between the introduced negatively charges and the acidic residues on the TRAP tail on our data.

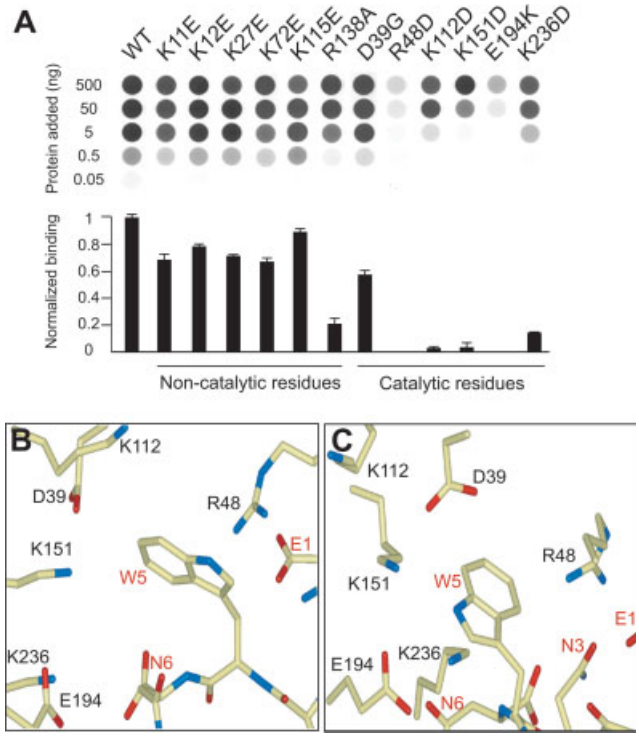

Fig. 5. Binding of PfAldo site-specific mutants to TRAP. (**A**) Different amounts of each PfAldo mutant (indicated above in single letter amino acid code) were added to TRAP 25mer peptide-coated plates, and the binding was revealed by an antibody against the Plasmodium aldolase C-terminal peptide followed by chemolluminescent detection. Signal quantitation is indicated in the lower panel. Panels (**B**) and (**C**) show two different close-up views of the lowest energy configuration of the TRAP 6mer and the catalytic residues (both in stick depiction) mutated in panel (A). TRAP residues (in red) are indicated as in Figure 3.

DISCUSSION

Altogether, our results indicate that the extreme C-terminal portion of TRAP binds to the active site of PfAldo in a highly restrained fashion (Fig. 1). This model of interaction is supported by concordance between the site-directed mutagenesis results (Fig. 5) and the contact area measurements from the convergent docking found for the 6mer peptide (Table II) together with the results obtained for the 24mer peptide (data not shown). Consistent with previous binding data,[19,20] additional docking simulations using a TRAP-mutated peptide indicate that this interaction is likely driven by the TRAP n-1 Trp residue (Fig. 2). Even though the N-terminus of the TRAP 24mer peptide bears some acidic stretches that indeed contribute to the overall interaction with aldolase,[18] we were not able to achieve convergent docking for this longer peptide. This might be due to the large and flexible nature of the ligand, which adds internal degrees of freedom to the already enormous computational burden. Alternatively, it may indicate that the N-terminal region of the TRAP 24mer peptide binds in a disordered fashion to the enzyme surface, which might explain in part the failure of our previous cocrystallization trials using PfAldo and large TRAP peptides.[19]

In the best docking conformation, the backbone of the key n-1 Trp and the side-chain of the n-2 Asp residue almost juxtapose with the F1,6P location in aldolase-trapped crystallographic complexes (Fig. 3). In addition, the finding that >98% of the 200 most stable configurations were obtained from noncomplexed conformations of the PfAldo receptor (Suppl. Table I) indicates the existence of some conformational shift on the aldolase active site during substrate turnover, which is detrimental for the docking of the TRAP peptide. Together, these data strongly suggest that F1,6P (or DHAP, data not shown) and TRAP compete for the enzyme active site either by steric hindrance or, more likely, by direct competition for the anchoring residues, which may adopt different side-chain conformations to accommodate either ligand. This assumption is experimentally supported by our aldolase inhibition assays using both synthetic peptides and recombinant fusion proteins (Fig. 4), and by previous data showing the displacement of TRAP/WASp peptides by aldolase substrate/products.[18,19] The inhibition capacity of TRAP/WASp molecules seems to correlate with their apparent affinity, and it is strictly dependent on their Trp residues (Fig. 4).[18] Interestingly, it has been shown that phosphate derivatives of different aromatic compounds bind to the aldolase active site and inhibit enzymatic activity by acting as substrate analogs.[43,44] Overall, these results demonstrate that TRAP/WASp are competitive inhibitors, though very poor ones, of aldolase activity. As discussed before,[18] this kind of metabolic regulation mediated by F1,6P, DHAP, and G3P might be of functional relevance *in vivo*, at least in the case of the engagement of the Plasmodium sporozoite motor. Since these metabolites also inhibit the interaction between aldolase and F-actin,[19,45] they are ideally suited to prevent the formation of nonproductive associations between TRAP and "soluble," F-actin detached aldolase (for a review, see 21). The striking similarity between the binding/inhibitory features of TRAP and WASp to PfAldo (Fig. 4), and their *in vitro* competition,[18] strongly suggest that WASp is also targeting the aldolase active site. The similar binding profile of WASp and TRAP to mutant PfAldo molecules further supports this idea (Suppl. Fig. 3).

The flexible docking technology used in this study has been originally established for the identification of the binding energies between phosphotyrosine-containing peptides and Src homology 2 (SH2)/phosphotyrosine-binding domains.[46] Further refinements of this approach allowed for the successful prediction of antibody–antigen and peptide–MHC interactions in a completely automatic, unrestrained fashion, and displayed an overall 89% of accuracy in the prediction of the binding location of protein complexes under blind conditions.[34,47] Here, besides algorithms[48] to account for induced fit in the side-chains of the genuine PfAldo structure,[2] we used additional *in silico* receptors modeled upon different crystallographic structures of evolutionarily related molecules (Table I). Interestingly, the 50 lowest energy conformations were obtained with a high resolution (1.8 Å) PfAldo homology

model derived from the *L. mexicana* aldolase structure[3] rather than from PfAldo itself (Suppl. Table I). Incorporating backbone flexibility into docking predictions is an unsolved problem. Docking to an ensemble of crystallographic or NMR conformations of the same protein can and has accounted for backbone flexibility in such predictions, but the novel approach used in this work demonstrated that, in some cases, docking to an ensemble of structures derived from evolutionary homologs (>45% identity in this study) may encode backbone deviations that enhance docking results (Suppl. Fig. 1). The high resolution of the homologous structure may have also been required to successfully transmit valuable backbone flexibility structural information to the approach. Conversely, the relatively low resolution (3.0 Å) of the available PfAldo structure may have limited its value as a docking receptor, and it is unclear whether a higher resolution would have supported a similar productive docking study without the need for homology models of other forms. Thus, in a case like this one, where only a low resolution target is available, the docking protocol we used may productively incorporate backbone flexibility into the docking prediction.

The overall mutational data strongly support the flexible docking-based structural model (Fig. 5 and Table II). The possibility that single residue substitutions in the PfAldo catalytic pocket cause extensive protein unfolding accounting for the diminished TRAP binding is very unlikely and could not be observed in other mutational studies using different aldolases.[16,42] Furthermore, some of the active site mutants showing significantly impaired binding to TRAP retained the overall quaternary structure (Suppl. Fig. 2). Although the mutations to glycine of Arg 48 and Lys 151 might have led to an unexpected flexibility on the PfAldo active site (and, indirectly, to a loss of TRAP binding), our data suggests that the effects we observe are direct. Firstly, mutation of the neighboring active site residue Asp 39 to Gly had no major effect on TRAP binding despite abolishing PfAldo enzymatic activity (Fig. 5). Secondly, indistinguishable results were obtained when Lys151 and Arg48 were mutated to either Asp or Gly. More importantly, on the basis of the identity of our ligand, mutation of Lys 151 and Arg 48 residues to Gly instead of Ala minimizes possible nonspecific hydrophobic interactions between the PfAldo active site and the sub-terminal Trp of the TRAP peptide, which is critical for this binding.

The only discrepancy between the docking and the mutagenesis results was found for the active site residue Asp 39. However, since the lowest energy configurations showed very similar energy scores (Suppl. Table I), and basically the same position and direction of the TRAP peptide into the PfAldo active site [Fig. 1(B)], it is therefore possible that different subsets of the atomic contacts between TRAP and PfAldo are equally energetically favorable to formation of the complex. Indeed, it is unlikely that the native crystallographic receptor conformation of PfAldo bound to TRAP would be identical throughout the peptide interaction surface as one of the conformations used here. The docked conformation may indeed exhibit one (Asp 39) out of many mutagenically proven non-native contacts without being globally inaccurate. The converse, and more serious, discrepancy was nevertheless not observed: none of the active site residues showing a strong effect on binding by mutagenesis were noted to be out of contact with the docked conformation of TRAP. In conclusion, the bulk of the data presented herein along with (1) the docking preference of the n-1 Trp side-chain conformations in all six PfAldo receptor models derived from noncomplexed crystallographic structures and (2) the strong structural conservation of the surface to which the Trp side-chain binds in these docking receptors, support the accuracy of the docking. More distal, surrounding protein surfaces, which vary more between the various homologs, are likely responsible for the few discrepancies observed here. Most importantly, our results might help in refining the conditions for the on-going cocrystallization trials between TRAP and PfAldo (e.g. by defining a proper TRAP peptide length) and, by identifying at least the general binding location of TRAP on PfAldo, might provide avenues for designing drugs to treat malaria and other diseases caused by apicomplexan parasites.

ACKNOWLEDGMENTS

We thank Dr. Claudia Roach (University of Washington, Seattle) for her assistance in the first mutation experiments and Dr. Jüergen Bosch (University of Washington, Seattle) for stimulating discussions. We are also indebted to Dr. María del Pilar Molina Portela (NYU) for some of the FPLC runs and to Mingyuan Tao (NYU) for his technical assistance.

REFERENCES

1. Gefflaut T, Blonski C, Perie J, Willson M. Class I aldolases: substrate specificity, mechanism, inhibitors and structural aspects. Prog Biophys Mol Biol 1995;63:301–340.
2. Kim H, Certa U, Dobeli H, Jakob P, Hol WG. Crystal structure of fructose-1,6-bisphosphate aldolase from the human malaria parasite *Plasmodium falciparum*. Biochemistry 1998;37:4388–4396.
3. Chudzik DM, Michels PA, de Walque S, Hol WG. Structures of type 2 peroxisomal targeting signals in two trypanosomatid aldolases. J Mol Biol 2000;300:697–707.
4. Hester G, Brenner-Holzach O, Rossi FA, Struck-Donatz M, Winterhalter KH, Smit JD, Piontek K. The crystal structure of fructose-1,6-bisphosphate aldolase from *Drosophila melanogaster* at 2.5 Å resolution. FEBS Lett 1991;292:237–242.
5. Gamblin SJ, Davies GJ, Grimes JM, Jackson RM, Littlechild JA, Watson HC. Activity and specificity of human aldolases. J Mol Biol 1991;219:573–576.
6. Dalby AR, Tolan DR, Littlechild JA. The structure of human liver fructose-1,6-bisphosphate aldolase. Acta Crystallogr D Biol Crystallogr 2001;57:1526–1533.
7. Arakaki TL, Pezza JA, Cronin MA, Hopkins CE, Zimmer DB, Tolan DR, Allen KN. Structure of human brain fructose 1,6-(bis)phosphate aldolase: linking isozyme structure with function. Protein Sci 2004;13:3077–3084.
8. Dalby A, Dauter Z, Littlechild JA. Crystal structure of human muscle aldolase complexed with fructose 1,6-bisphosphate: mechanistic implications. Protein Sci 1999;8:291–297.
9. Choi KH, Mazurkie AS, Morris AJ, Utheza D, Tolan DR, Allen KN. Structure of a fructose-1,6-bis(phosphate) aldolase liganded to its natural substrate in a cleavage-defective mutant at 2.3 Å. Biochemistry 1999;38:12655–12664.

10. Choi KH, Shi J, Hopkins CE, Tolan DR, Allen KN. Snapshots of catalysis: the structure of fructose-1,6-(bis)phosphate aldolase covalently bound to the substrate dihydroxyacetone phosphate. Biochemistry 2001;40:13868–13875.
11. St-Jean M, Lafrance-Vanasse J, Liotard B, Sygusch J. High resolution reaction intermediates of rabbit muscle fructose-1,6-bisphosphate aldolase: substrate cleavage and induced fit. J Biol Chem 2005;280:27262–27270.
12. Sygusch J, Beaudry D, Allaire M. Molecular architecture of rabbit skeletal muscle aldolase at 2.7 Å resolution. Proc Natl Acad Sci USA 1987;84:7846–7850.
13. Berthiaume L, Tolan DR, Sygusch J. Differential usage of the carboxyl-terminal region among aldolase isozymes. J Biol Chem 1993;268:10826–10835.
14. Blom N, Sygusch J. Product binding and role of the C-terminal region in class I D-fructose 1,6-bisphosphate aldolase. Nat Struct Biol 1997;4:36–39.
15. O'Reilly G, Clarke F. Identification of an actin binding region in aldolase. FEBS Lett 1991;321:69–72.
16. Wang J, Morris AJ, Tolan DR, Pagliaro L. The molecular nature of the F-actin binding activity of aldolase revealed with site-directed mutants. J Biol Chem 1996;271:6861–6865.
17. Carr D, Knull H. Aldolase-tubulin interactions: removal of tubulin C-terminals impairs interactions. Biochem Biophys Res Commun 1993;195:289–293.
18. Buscaglia CA, Penesetti D, Tao M, Nussenzweig V. Characterization of an aldolase-binding site in the Wiskott–Aldrich syndrome protein. J Biol Chem 2006;281:1324–1331.
19. Buscaglia CA, Coppens I, Hol WG, Nussenzweig V. Sites of interaction between aldolase and thrombospondin-related anonymous protein in plasmodium. Mol Biol Cell 2003;14:4947–4957.
20. Jewett TJ, Sibley LD. Aldolase forms a bridge between cell surface adhesins and the actin cytoskeleton in apicomplexan parasites. Mol Cell 2003;11:885–894.
21. Kappe SH, Buscaglia CA, Bergman LW, Coppens I, Nussenzweig V. Apicomplexan gliding motility and host cell invasion: overhauling the motor model. Trends Parasitol 2004;20:13–16.
22. Soldati D, Foth BJ, Cowman AF. Molecular and functional aspects of parasite invasion. Trends Parasitol 2004;20:567–574.
23. Kappe S, Bruderer T, Gantt S, Fujioka H, Nussenzweig V, Menard R. Conservation of a gliding motility and cell invasion machinery in Apicomplexan parasites. J Cell Biol 1999;147:937–944.
24. Baum J, Richard D, Healer J, Rug M, Krnajski Z, Gilberger TW, Green JL, Holder AA, Cowman AF. A conserved molecular motor drives cell invasion and gliding motility across malaria life cycle stages and other Apicomplexan parasites. J Biol Chem 2006;281:5197–5208.
25. Menard R. Gliding motility and cell invasion by Apicomplexa: insights from the Plasmodium sporozoite. Cell Microbiol 2001;3:63–73.
26. Sibley LD. Intracellular parasite invasion strategies. Science 2004;304:248–253.
27. Gaffar FR, Yatsuda AP, Franssen FF, de Vries E. A *Babesia bovis* merozoite protein with a domain architecture highly similar to the thrombospondin-related anonymous protein (TRAP) present in Plasmodium sporozoites. Mol Biochem Parasitol 2004;136:25–34.
28. Jones ML, Kitson EL, Rayner JC. *Plasmodium falciparum* erythrocyte invasion: a conserved myosin associated complex. Mol Biochem Parasitol 2006;147:74–84.
29. Schneider ML, Post CB. Solution structure of a band 3 peptide inhibitor bound to aldolase: a proposed mechanism for regulating binding by tyrosine phosphorylation. Biochemistry 1995;34:16574–16584.
30. Murzin AG, Brenner SE, Hubbard T, Chothia C. SCOP: a structural classification of proteins database for the investigation of sequences and structures. J Mol Biol 1995;247:536–540.
31. Cardozo T, Totrov M, Abagyan R. Homology modeling by the ICM method. Proteins 1995;23:403–414.
32. Abagyan R, Totrov M. Biased probability Monte Carlo conformational searches and electrostatic calculations for peptides and proteins. J Mol Biol 1994;235:983–1002.
33. Totrov M, Abagyan R. Flexible protein–ligand docking by global energy optimization in internal coordinates. Proteins 1997;(Suppl. 1):215–220.
34. Bordner AJ, Abagyan R. Ab initio prediction of peptide-MHC binding geometry for diverse class I MHC allotypes Proteins 2006;63:512–514.
35. Fernandez-Recio J, Totrov M, Abagyan R. Soft protein–protein docking in internal coordinates. Protein Sci 2002;11:280–291.
36. Nemethy G, Gibson KD, Palmer KA, Yoon CN, Paterlini G, Zagari A, Rumsey S, Scherag HA. Energy parameters in polypeptides, Part 10: Improved geometrical parameters and nonbonded interactions for use in the ECEPP/3 algorithm, with application to proline-containing peptides. J Phys Chem 1992;96:6472–6484.
37. Totrov M, Abagyan R. Detailed ab initio prediction of lysozyme-antibody complex with 1.6 Å accuracy. Nat Struct Biol 1994;1:259–263.
38. Abagyan R, Argos P. Optimal protocol and trajectory visualization for conformational searches of peptides and proteins. J Mol Biol 1992;225:519–532.
39. Metropolis NA, Rosenbluth AW, Rosenbluth NM, Teller AH, Teller E. Equation of state calculations by fast computing machines. J Chem Phys 1953;21:1087–1092.
40. Knapp B, Hundt E, Kupper HA. *Plasmodium falciparum* aldolase: gene structure and localization. Mol Biochem Parasitol 1990;40:1–4.
41. Alvarez P, Buscaglia CA, Campetella O. Improving protein pharmacokinetics by genetic fusion to simple amino acid sequences. J Biol Chem 2004;279:3375–3381.
42. Maurady A, Zdanov A, de Moissac D, Beaudry D, Sygusch J. A conserved glutamate residue exhibits multifunctional catalytic roles in D-fructose-1,6-bisphosphate aldolases. J Biol Chem 2002;277:9474–9483.
43. Blonski C, De Moissac D, Perie J, Sygusch J. Inhibition of rabbit muscle aldolase by phosphorylated aromatic compounds. Biochem J 1997;323:71–77.
44. Dax C, Coincon M, Sygusch J, Blonski C. Hydroxynaphthaldehyde phosphate derivatives as potent covalent Schiff base inhibitors of fructose-1,6-bisphosphate aldolase. Biochemistry 2005;44:5430–5443.
45. Schindler R, Weichselsdorfer E, Wagner O, Bereiter-Hahn J. Aldolase-localization in cultured cells: cell-type and substrate-specific regulation of cytoskeletal associations. Biochem Cell Biol 2001;79:719–728.
46. Zhou Y, Abagyan R. How and why phosphotyrosine-containing peptides bind to the SH2 and PTB domains. Fold Des 1998;3:513–522.
47. Fernandez-Recio J, Abagyan R, Totrov M. Improving CAPRI predictions: optimized desolvation for rigid-body docking. Proteins 2005;60:308–313.
48. Fernandez-Recio J, Totrov M, Abagyan R. ICM-DISCO docking by global energy optimization with fully flexible side-chains. Proteins 2003;52:113–117.